LOCALIZED RANDOM SAMPLING FOR ROBUST COMPRESSIVE BEAM ALIGNMENT

Nitin Jonathan Myers and Robert W. Heath Jr.

Department of Electrical and Computer Engineering, The University of Texas at Austin.

email: {nitinjmyers, rheath}@utexas.edu

ABSTRACT

Compressed sensing (CS)-based beam alignment is a promising solution for rapid link configuration in millimeter wave (mmWave) systems that use large arrays. Translating CS to practical mmWave radios, however, can be challenging due to carrier frequency offset (CFO). Standard sparse recovery techniques that use random sampling strategies to acquire channel measurements can fail even if there is a slight mismatch in carrier frequencies. In this paper, we show that restricting the randomness in compressive sampling to local sets can achieve robustness to structured errors due to CFO. The proposed approach requires fewer channel measurements than comparable algorithms and has the same complexity as standard CS.

Index Terms— Robust beamforming, mm-Wave, carrier frequency offset, robust compressed sensing

1. INTRODUCTION

Next generation wireless systems will exploit the large amount of spectrum available at mmWave carrier frequencies [1]. Although today's circuit technology can support communication at mmWave, it comes with a lot of challenges from a signal processing perspective. For example, the use of fewer number of radio frequency (RF) chains than antennas results in limited access to the radio channel [2]. The phased antenna array with a single RF chain is one example of an hardware architecture that is commonly used at mmWave [3]. Using a phased array, the transmitter (TX) and the receiver (RX) can perform directional transmission and reception by appropriately configuring their phase shifters [2]. The objective of beam alignment is to determine the best phase shift configurations at the TX and the RX that maximize the received SNR [3]. Unfortunately, standard exhaustive scan-based beam alignment, in which the TX and the RX scan all potential directions in the channel, incurs substantial training overhead in mmWave systems with large arrays [4].

Compressive sensing recovers a sparse signal from fewer linear measurements of the signal compared to its dimension [5]. As mmWave channels are sparse in a well-chosen dictionary, CS has been extensively applied for faster mmWave channel estimation and beam alignment [6][7]. Most of the existing CS-based techniques, however, assume that CFO has been perfectly corrected. Such an assumption may not be valid in typical mmWave settings as perfect CFO correction can be hard due to low SNR prior to initial beamforming [2]. CS-based techniques that account for CFO either have high complexity [8] or ignore the structure in the phase errors [4].

In this paper, we define the notion of robustness for compressive beam alignment, by identifying a set of sparse channels around the true channel that are acceptable for beam alignment. Then, we develop a sampling strategy for compressive channel acquisition such that standard CS under a CFO error provides a channel estimate within the acceptable set. CS with the proposed sampling technique results in smaller beam misalignments when compared to the common random phase shift-based CS [7]. We show how beam broadening can be used to compensate for such small misalignments. Simulation results show that our approach achieves a reasonable beamforming gain over a wider range of CFO when compared to beam alignment through random phase shift-based CS.

Notation: A is a matrix, **a** is a column vector and a, A denote scalars. The matrices $\mathbf{A}^T, \overline{\mathbf{A}}$ and \mathbf{A}^* represent the transpose, conjugate and conjugate transpose of \mathbf{A} . The scalar a [m] denotes the m^{th} element of \mathbf{a} . The (k,ℓ) entry of \mathbf{A} is $\mathbf{A}(k,\ell)$ or $A_{k,\ell}$. The ℓ^{th} column of \mathbf{A} is $\mathbf{A}(:,\ell)$. The matrix $|\mathbf{A}|$ contains the element-wise magnitude of the entries of \mathbf{A} . The symbol \odot denotes the Hadamard product. I denotes the identity matrix and $\mathbf{U}_N \in \mathbb{C}^{N \times N}$ denotes the unitary Discrete Fourier Transform (DFT) matrix. We use \mathbf{e}_k to represent the $(k+1)^{\mathrm{th}}$ canonical basis vector. The set \mathcal{I}_N denotes the set of integers $\{0,1,2,...,N-1\}$.

2. SYSTEM AND CHANNEL MODEL

We consider a mmWave system with a uniform linear array (ULA) of N antennas at the TX and the RX. Both the TX and RX are equipped with a phased antenna array architecture [2]. Each of the N transmit antennas are connected to the RF chain at the TX using a q-bit phase shifter. Similarly, each receive antenna is connected to the RF chain at the RX using a q-bit phase shifter. The TX and the RX can control their phase shifters by applying beamforming vectors to their phased arrays [3]. Beam alignment determines the best beamforming vectors at the TX and the RX that maximize the received SNR. The best beamforming vectors depend on the multiple-input multiple-output (MIMO) channel between the TX and the RX.

The narrowband mmWave MIMO channel, defined as $\mathbf{H} \in \mathbb{C}^{N \times N}$, can be estimated by acquiring channel measurements using pre-defined beam training vectors at the TX and the RX. We use M to denote the number of channel measurements acquired to learn \mathbf{H} . For $\alpha = 1/\sqrt{N}$ and $\theta_i = 2\pi i/2^q$, we define $\mathbb{Q}_q = \left\{\alpha e^{j\theta_1}, \alpha e^{j\theta_2}, ..., \alpha e^{j\theta_{2q}}\right\}$ as a set of allowed phase shifts. To obtain the m^{th} channel measurement, the TX and the RX apply $\mathbf{f}[m] \in \mathbb{Q}_q^N$ and $\mathbf{w}[m] \in \mathbb{Q}_q^N$ to their phased arrays. Let ϵ be the digital domain CFO that corrupts the phase of the received signal. Specifically, for a CFO of Δf in the analog domain and a symbol duration of T, we have $\epsilon = 2\pi\Delta fT$. The m^{th} channel measurement acquired by the RX can be expressed as [8]

$$y[m] = \mathbf{w}^*[m]\mathbf{H}\overline{\mathbf{f}}[m]e^{\mathbf{j}\epsilon m} + v[m], \tag{1}$$

where v[m] is additive white Gaussian noise with zero mean and a variance of σ^2 . The model in (1) assumes a narrowband setting with perfect frame timing synchronization and ignores phase noise. Relaxing these assumptions is an interesting direction for future work.

This material is based upon work supported in part by the National Science Foundation under Grant No. CNS-1702800 and ECCS-1711702.

In a ULA-based system, the mmWave channel is approximately sparse in the 2D-discrete Fourier transform (2D-DFT) dictionary due to clustering in the propagation environment [2]. We define the beamspace channel \mathbf{X} as the 2D-DFT of \mathbf{H} [9]:

$$\mathbf{H} = \mathbf{U}_N^* \mathbf{X} \mathbf{U}_N^*. \tag{2}$$

For a tractable analysis, we consider X to be perfectly sparse, and evaluate our design for a practical mmWave setting where X is approximately sparse. The matrix X is also called as the angle domain channel, as the vertical and horizontal dimensions of the beamspace correspond to the receive and transmit directions in the channel. A common approach to perform beam alignment is one that uses the maximizer of **X**, i.e., the 2D coordinate $(r_{\text{opt}}, c_{\text{opt}})$ where $|\mathbf{X}|$ achieves its maximum. These coordinates correspond to beamspace directions of $2\pi r_{\rm opt}/N$ and $2\pi c_{\rm opt}/N$ at the RX and the TX. Beam alignment along these directions is performed by using the q-bit phase quantized versions of $\overline{\mathbf{U}}_N(:,r_{\mathrm{opt}})$ and $\overline{\mathbf{U}}_N(:,c_{\mathrm{opt}})$ as the beamforming vectors at the RX and the TX. As perfect channel state information (CSI) is not available in practice, beam alignment can be performed using an estimate of X, or equivalently H. It can be observed from (1) that $M = N^2$ channel measurements are needed to estimate a generic channel **H** in the absence of CFO. For $\epsilon = 0$, CS-based techniques that exploit sparsity of the mmWave channel in the 2D-DFT dictionary can recover X from $M \ll N^2$ channel measurements [6][7].

CFO corrupts the phase of the channel measurements in (1). The phase error due to CFO linearly increases with m, i.e., the index of the acquired channel measurement, and is unknown. Standard CS with the common independent and identically distributed (IID) random phase shift-based channel acquisition [7] may fail to recover the sparse channel when $\epsilon \neq 0$. This paper focusses on the design of beam training vectors $\{(\mathbf{f}[m],\mathbf{w}[m])\}_{m=0}^{M-1}$ such that standard CS with the proposed design is robust to phase errors due to ϵ when compared to the random phase shift-based design.

3. LIMITING RANDOMNESS FOR ROBUST CS

For a tractable design of beam training vectors for robust CS, we consider a special class of CS called convolutional CS (CCS) [10]. Let $\mathbf{z} \in \mathbb{Q}_q^N$ be the modulation sequence used for CCS of **H** [11]. In CCS, the TX and the RX can only apply circulantly shifted versions of z as the beam training vectors for channel acquisition. As N distinct circulant shifts of z can be applied, there are N candidate beam training vectors that can be used at each of the TX and the RX in CCS. We define a right circulant delay matrix $\mathbf{J} \in \mathbb{R}^{N \times N}$ such that its first row is (0, 1, 0, ..., 0). The subsequent rows of **J** are right circulant shifted versions of the previous row by one unit. The ℓ circulant delay matrix is defined as $\mathbf{J}_{\ell} = \mathbf{J} \cdot \mathbf{J} \cdots \mathbf{J}$ (ℓ times). We define $J_0 = I$ and $J_{-\ell} = J_{N-\ell}$. We define $Z = [z, J_1z, J_2z, ..., J_{N-1}z]$. In CCS, the columns of **Z** are used as the beam training vectors. When $\ell_{\rm tx}[m]$ and $\ell_{\rm rx}[m]$ circulantly shifted versions of **z** are applied to the phased arrays at the TX and the RX, we have $\mathbf{f}[m] = \mathbf{Z}\mathbf{e}_{\ell_{\mathrm{tx}}[m]}$ and $\mathbf{w}[m] = \mathbf{Z}\mathbf{e}_{\ell_{\mathbf{rx}}[m]}$. As a result, the channel measurement in (1) can be expressed as

$$y[m] = \mathbf{e}_{\ell_{\text{rx}}[m]}^T \mathbf{Z}^* \mathbf{H} \overline{\mathbf{Z}} \mathbf{e}_{\ell_{\text{tx}}[m]} e^{\mathbf{j}\epsilon m} + v[m]. \tag{3}$$

For $\epsilon=0$, the entries of ${\bf Z}^*{\bf H}\overline{\bf Z}$ can be acquired one at a time by applying different amounts of circulant shifts at the TX and the RX. We define the pseudo-channel matrix as ${\bf G}={\bf Z}^*{\bf H}\overline{\bf Z}$. Using this definition, the channel measurement in (3) can be written as

$$y[m] = \mathbf{G}(\ell_{\rm rx}[m], \ell_{\rm tx}[m])e^{\mathrm{j}\epsilon m} + v[m]. \tag{4}$$

In a noiseless setting with zero CFO, G can be directly sampled using CCS unlike H, i.e., the true channel [11][12].

Now, we show that \mathbf{G} has the same structural property as \mathbf{H} when \mathbf{z} is chosen as a Zadoff-Chu (ZC) sequence. To illustrate the equivalence, we define a diagonal matrix $\Lambda_{\mathbf{z}}$ such that $\Lambda_{\mathbf{z}} = \mathbf{U}_N \mathbf{Z}^* \mathbf{U}_N^*$; this follows from the property that the DFT matrix can diagonalize the circulant matrix \mathbf{Z}^* . Analogous to the definition of the beamspace channel \mathbf{X} , we define a masked beamspace channel \mathbf{S} as the 2D-DFT of the pseudo-channel, i.e., $\mathbf{S} = \mathbf{U}_N \mathbf{G} \mathbf{U}_N$. Using $\mathbf{G} = \mathbf{Z}^* \mathbf{H} \overline{\mathbf{Z}}$, $\mathbf{H} = \mathbf{U}_N^* \mathbf{X} \mathbf{U}_N^*$, and $\mathbf{U}_N \mathbf{Z}^* \mathbf{U}_N^* = \mathbf{\Lambda}_{\mathbf{z}}$, we can write

$$\mathbf{S} = \mathbf{\Lambda}_{\mathbf{z}} \mathbf{X} \mathbf{\Lambda}_{\mathbf{z}}.\tag{5}$$

When \mathbf{z} is chosen as a ZC sequence, the diagonal entries of $\mathbf{\Lambda}_{\mathbf{z}}$ are unimodular [11]. As a result, $|\mathbf{S}(k,\ell)| = |\mathbf{X}(k,\ell)|$ for every k and ℓ , and $|\mathbf{S}|$ achieves its maximum at $(r_{\mathrm{opt}}, c_{\mathrm{opt}})$. Therefore, \mathbf{S} can be used to perform beam alignment instead of \mathbf{X} . Note that the inverse 2D-DFT of the sparse matrix \mathbf{S} is \mathbf{G} . From standard CS theory [13], it can be concluded that \mathbf{S} can be reconstructed from $M = \mathcal{O}(\log N)$ random samples of \mathbf{G} for $\epsilon = 0$ [12].

When the phase of the samples acquired from ${\bf G}$ are perturbed due to CFO, standard CS results in a blurred and shifted version of ${\bf S}$ that may not be useful for beam alignment [12]. Such unknown shifts result in mismatched beamforming, i.e., the matrix $\hat{{\bf S}}$ obtained with standard CS may achieve its maximum at $(r_{\rm opt}+\delta_1,c_{\rm opt}+\delta_2)$ for some $\delta_1\neq 0$ and $\delta_2\neq 0$. The directional perturbations, i.e., $2\pi\delta_1/N$ and $2\pi\delta_2/N$ can be very large for the IID phase shift-based design [12]. Our approach for robust CS-based beam alignment consists of two components. The first component in Sec. 3.1 and Sec. 3.2, designs a sampling scheme for CS such that CFO results in small bounded beam misalignments when compared to those resulting from the random phase shift-based design. The second component in Sec. 3.3, develops a beam broadening strategy that compensates for the bounded beam misalignments.

3.1. Robustness in the context of beam alignment

A reasonable requirement for robust CS is that a CFO of ϵ should result in beam misalignments that are no more than ϵ at both the TX and the RX. In most wireless systems, the CFO is bounded by some Δ , i.e., $|\epsilon| \leq \Delta$. Under the requirement for robust CS, we can be sure that the estimated transmit and receive directions deviate from the true directions by a maximum of Δ radians. The proposed robust CS technique is useful as CS with the common random phase shift-based training can result in misalignments that can be larger than Δ . For our analysis, we assume that ϵ and Δ are integer multiples of $2\pi/N$ to define $n_{\epsilon} = N\epsilon/(2\pi)$ and $u = N\Delta/(2\pi)$. For a maximum CFO of Δ , the set of acceptable masked beamspace channels around S is defined as

$$S(\Delta, \mathbf{S}) = \{ \mathbf{R} : \mathbf{R} = \mathbf{J}_{t_{\text{rx}}} \mathbf{S} \mathbf{J}_{t_{\text{tx}}}^T, |t_{\text{rx}}| \le u, \text{ and } |t_{\text{tx}}| \le u \}.$$
 (6)

For any $\tilde{\mathbf{S}} \in \mathcal{S}(\Delta, \mathbf{S})$, it can be observed from (6) that the maximizers of $\tilde{\mathbf{S}}$ and \mathbf{S} differ (in modulo N) by a maximum of u units along both the row and column dimensions. In beamspace terms, the best directions corresponding to $\tilde{\mathbf{S}}$ and \mathbf{S} can differ by a maximum of $2\pi u/N$ units. By our definition, a robust CS technique is one that provides any matrix within the acceptable set, i.e., $\mathcal{S}(\Delta, \mathbf{S})$.

For tractability of robust CS design, we consider a special case of $t_{\rm rx}=t_{\rm tx}$ in (6). We define $\mathcal{S}_o(\Delta,\mathbf{S})\subset\mathcal{S}(\Delta,\mathbf{S})$ such that $\mathcal{S}_o(\Delta,\mathbf{S})=\{\mathbf{R}:\mathbf{R}=\mathbf{J}_t\mathbf{S}\mathbf{J}_t^T,|t|\leq u\}$, and $\mathcal{G}_o(\Delta,\mathbf{S})=\{\mathbf{P}:\mathbf{P}=\mathbf{U}_N^*\mathbf{R}\mathbf{U}_N^*$ for $\mathbf{R}\in\mathcal{S}_o(\Delta,\mathbf{S})\}$ as a set that contains the inverse 2D-DFT of all the elements in $\mathcal{S}_o(\Delta,\mathbf{S})$. As $\mathbf{S}\in\mathcal{S}_o(\Delta,\mathbf{S})$

and $\mathbf{G} = \mathbf{U}_N^* \mathbf{S} \mathbf{U}_N^*$, it follows that $\mathbf{G} \in \mathcal{G}_o(\Delta, \mathbf{S})$. A graphical illustration of the sets is shown in Fig. 1. Relaxing the condition $t_{\mathrm{rx}} = t_{\mathrm{tx}}$ to develop new robust CS techniques is an interesting direction for future work. Now, we investigate the possibility of using CS to recover a matrix in $\mathcal{S}_o(\Delta, \mathbf{S})$. As circulant shifts of a signal do not change its sparsity, any matrix in $\mathcal{S}_o(\Delta, \mathbf{S})$ is sparse as \mathbf{S} is sparse. As partial 2D-DFT CS can estimate \mathbf{S} from fewer samples of \mathbf{G} for $\epsilon = 0$, a natural question to ask is if partial 2D-DFT CS can recover any $\mathbf{R} \in \mathcal{S}_o(\Delta, \mathbf{S})$ using subsamples of some $\mathbf{P} \in \mathcal{G}_o(\Delta, \mathbf{S})$. Note that subsamples of \mathbf{G} cannot be acquired when $\epsilon \neq 0$.

To characterize matrices in $\mathcal{G}_o(\Delta, \mathbf{S})$, we define a Vandermonde vector $\mathbf{a}_N(\theta) = (1, e^{\mathrm{j}\theta}, e^{\mathrm{j}2\theta}, \dots, e^{\mathrm{j}(N-1)\theta})^T$ and a matrix $\mathbf{A}_N(\theta) = \mathbf{a}_N(\theta)\mathbf{a}_N^T(\theta)$. We claim that $\mathbf{G}\odot\mathbf{A}_N(\epsilon)\in\mathcal{G}_o(\Delta,\mathbf{S})$ for any $|\epsilon|\leq \Delta$, and show that subsamples of such a matrix can be acquired by the RX in Sec. 3.2. The masked beamspace matrix corresponding to $\mathbf{G}\odot\mathbf{A}_N(\epsilon)$ is $\mathbf{U}_N(\mathbf{G}\odot\mathbf{A}_N(\epsilon))\mathbf{U}_N$. By the multiplication-convolution duality of the Fourier transform [14], it can be shown that the partial 2D-DFT of $\mathbf{G}\odot\mathbf{A}_N(\epsilon)$ is $\mathbf{J}_{n_\epsilon}\mathbf{S}\mathbf{J}_{n_\epsilon}^T$ as $\epsilon=2\pi n_\epsilon/N$. As $|n_\epsilon|\leq u$, $\mathbf{J}_{n_\epsilon}\mathbf{S}\mathbf{J}_{n_\epsilon}^T\in\mathcal{S}_o(\Delta,\mathbf{S})$. Therefore, $\mathbf{G}\odot\mathbf{A}_N(\epsilon)\in\mathcal{G}_o(\Delta,\mathbf{S})$. Now, sampling strategies that acquire subsamples of $\mathbf{G}\odot\mathbf{A}_N(\epsilon)$ must be developed so that 2D-DFT CS using these samples provides the sparse matrix $\mathbf{J}_{n_\epsilon}\mathbf{S}\mathbf{J}_{n_\epsilon}^T$.

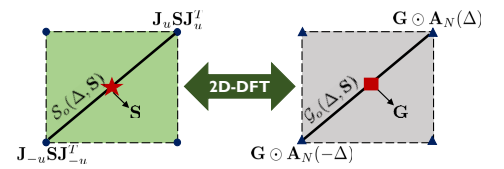


Fig. 1. The solid line on the left denotes $S_o(\Delta, \mathbf{S})$, i.e., the set of sparse matrices around \mathbf{S} that satisfy the notion of robustness for beam alignment. $\mathcal{G}_o(\Delta, \mathbf{S})$ contains the 2D-DFT of all the elements in $\mathcal{S}_o(\Delta, \mathbf{S})$. The extreme point $\mathbf{J}_u\mathbf{S}\mathbf{J}_u^T$ in $\mathcal{S}_o(\Delta, \mathbf{S})$ is the 2D-DFT of the extreme point $\mathbf{G}\odot\mathbf{A}_N(\Delta)$ in $\mathcal{G}_o(\Delta, \mathbf{S})$.

3.2. Proposed sampling technique

In this section, we show how subsamples of $G \odot A_N(\epsilon)$ can be acquired using the model in (4). The entries in $G \odot A_N(\epsilon)$ are

$$\begin{pmatrix} G_{0,0} & G_{0,1}e^{\mathrm{j}\epsilon} & G_{0,2}e^{2\mathrm{j}\epsilon} \cdots & G_{0,N-1}e^{\mathrm{j}(N-1)\epsilon} \\ G_{1,0}e^{\mathrm{j}\epsilon} & G_{1,1}e^{2\mathrm{j}\epsilon} & & G_{1,N-1}e^{\mathrm{j}N\epsilon} \\ G_{2,0}e^{2\mathrm{j}\epsilon} & \vdots & \ddots & \ddots & G_{2,N-1}e^{\mathrm{j}(N+1)\epsilon} \\ \vdots & & & \vdots \\ G_{N-1,0}e^{\mathrm{j}(N-1)\epsilon}G_{N-1,1}e^{\mathrm{j}N\epsilon} & \cdots & \cdots G_{N-1,N-1}e^{\mathrm{j}2(N-1)\epsilon} \end{pmatrix}$$

We sequentially substitute m=0,1,2,...,2N-2 in (4) to check which entries of $\mathbf{G}\odot\mathbf{A}_N(\epsilon)$ can be acquired by the RX. For m=0, it can be observed that the (0,0) entry of $\mathbf{G}\odot\mathbf{A}_N(\epsilon)$ can be sampled by using $\ell_{\mathrm{rx}}[0]=0$ and $\ell_{\mathrm{tx}}[0]=0$ in (4). Specifically, $G_{0,0}$ is acquired as the first channel measurement, i.e., for m=0, by using \mathbf{z} as the beam training vector at both the TX and the RX. For the second channel measurement, i.e., m=1, the CFO introduces a phase error of ϵ as seen in (4). Now, there are two entries in $\mathbf{G}\odot\mathbf{A}_N(\epsilon)$ that have a phase error of ϵ , i.e., at locations (1,0) and (0,1). To acquire $\mathbf{G}\odot\mathbf{A}_N(\epsilon)$ at (1,0), the RX and the TX must apply $\ell_{\mathrm{rx}}[1]=1$ and $\ell_{\mathrm{tx}}[1]=0$ circulant shifts of \mathbf{z} to their phased arrays. Similarly, the (0,1) entry of $\mathbf{G}\odot\mathbf{A}_N(\epsilon)$ can be acquired by using $\ell_{\mathrm{rx}}[1]=0$ and $\ell_{\mathrm{tx}}[1]=1$. For a particuar m, however, only one combination of beam training vectors can be used at the TX and the RX to obtain y[m]. Therefore, $(\ell_{\mathrm{rx}}[1],\ell_{\mathrm{tx}}[1])$ is chosen at random

from $\{(1,0),(0,1)\}$ and the corresponding pair of beam training vectors, i.e., $(\mathbf{Ze}_{\ell_{\mathsf{Tx}}[1]},\mathbf{Ze}_{\ell_{\mathsf{tx}}[1]})$, is used to obtain y[1]. For m=2, it can be observed that there are three terms in $\mathbf{G}\odot\mathbf{A}_N(\epsilon)$ that have a phase error of $e^{\mathbf{j}^{2\epsilon}}$. As the RX can acquire a single sample at m=2, one of the three coordinates in $\{(2,0),(1,1)(0,2)\}$ is chosen at random to define the beam training vectors. This process is stopped when the (N-1,N-1) coordinate of $\mathbf{G}\odot\mathbf{A}_N(\epsilon)$ is reached for m=2N-2. Thus, a maximum of 2N-1 samples of $\mathbf{G}\odot\mathbf{A}_N(\epsilon)$ can be acquired using the proposed strategy. The proposed beam training vector design technique, for $M\leq 2N-1$, is summarized in Algorithm 1.

```
\begin{array}{l} \text{for } m=0 \text{ to } M-1 \text{ do} \\ \textbf{1. Sample a coordinate at random from} \\ \{(a,b): a+b=m, a\in \mathcal{I}_N, b\in \mathcal{I}_N\} \\ \textbf{2. Define the sampled coordinate as } (\ell_{\text{rx}}[m],\ell_{\text{tx}}[m]) \\ \textbf{3. Set } \mathbf{w}[m] = \mathbf{Z}\mathbf{e}_{\ell_{\text{rx}}[m]} \text{ and } \mathbf{f}[m] = \mathbf{Z}\mathbf{e}_{\ell_{\text{tx}}[m]} \\ \textbf{end for} \end{array}
```

Algorithm 1: Proposed beam training vectors for robust CS

The randomness in sampling using our framework is constrained to local sets of m+1 coordinates for $m \leq N-1$, and 2N-1-m coordinates for $N \leq m \leq 2N-2$. At this point, we hope that CS can fill the unsampled entries of $\mathbf{G}\odot\mathbf{A}_N(\epsilon)$ by exploiting the sparsity of 2D-DFT of $\mathbf{G}\odot\mathbf{A}_N(\epsilon)$. Simulation results indicate that CS indeed recovers $\mathbf{G}\odot\mathbf{A}_N(\epsilon)$ or equivalently its 2D-DFT, i.e., $\mathbf{J}_{n_\epsilon}\mathbf{S}\mathbf{J}_{n_\epsilon}^T$, for a sufficiently large M that is smaller than 2N-1. For guarantees on the restricted isometry property of the CS matrix resulting from localized random subsampling and more elaborate simulations, we refer the interested reader to [12]. Swift-Link [12] considers planar arrays and uses the concept of trajectory to arrive at the proposed randomized subsampling scheme. In this paper, we approach the problem from a different perspective than Swift-Link, i.e., using the notion of robustness. As $\mathbf{J}_{n_\epsilon}\mathbf{S}\mathbf{J}_{n_\epsilon}^T\in\mathcal{S}_o(\Delta,\mathbf{S})$, standard CS using the proposed channel acquisition technique is robust to CFO.

3.3. Strategy to correct beam misalignments

CS with the proposed beam training design estimates $\mathbf{J}_{n_e} \mathbf{S} \mathbf{J}_{n_e}^T$, i.e., an $(n_{\epsilon}, n_{\epsilon})$ 2D-circulantly shifted version of S. The location that maximizes the estimated masked beamspace is then $(r_{\rm opt}+n_{\epsilon},c_{\rm opt}+n_{\epsilon})$. If CFO is ignored, the RX and the TX use directional beams defined by $r_{\rm est} = r_{\rm opt} + n_{\epsilon}$ and $c_{\rm est} = c_{\rm opt} + n_{\epsilon}$. Such a choice, however, may result in poor SNR. It can be observed that r_{opt} lies within u units of r_{est} as $|n_{\epsilon}| \leq u$. Therefore, broadening a directional beam along $2\pi r_{\rm est}/N$ by $2\pi u/N$ units on its either sides ensures that reasonable beamforming gain can be achieved along $2\pi r_{\rm opt}/N$. Finding beamforming vectors in \mathbb{Q}_a^N that results in a broadened beam, however, is non-trivial due to the constant magnitude of the elements in \mathbb{Q}_q^N . The beamforming vector corresponding to the broadened beam is obtained using the CAN algorithm in [15]. Let \mathbf{w}_{bd} and \mathbf{f}_{bd} be the broadened beamforming vectors used at the RX and the TX. The received SNR for such a configuration is $SNR_{bd} = |\mathbf{w}_{bd}^* \mathbf{H} \mathbf{\bar{f}}_{bd}|^2 / \sigma^2$. As the energy in the broadened transmit beam is distributed uniformly among 2u + 1directions, the energy of the beam along r_{opt} is 1/(2u+1). As a result, an SNR loss of $10\log_{10}(2u+1)$ dB is incurred with respect to the directional beam along $r_{\rm opt}$. The same amount of SNR loss is incurred due to beam broadening at the RX. Therefore, the total SNR loss relative to best directional transmission and reception is $20\log_{10}(2u+1)$ dB. As $u \ll N$ in typical mmWave systems, the SNR obtained with the broadened beams can still be significantly higher than that achieved by the omnidirectional one.

4. SIMULATIONS

We consider a narrowband mmWave system operating at a carrier frequency of 38 GHz. The symbol duration in the system is set as $T=10\,\mathrm{ns}$; this corresponds to a bandwidth of 100 MHz. A halfwavelength spaced linear array of N=64 antennas is used at both the TX and the RX. The resolution of the phase shifters in the antenna arrays at the TX and the RX is set as a = 3 bits. The channels in our simulation are generated from the NYUSIM simulator [16] for a urban micro line-of-sight (UMi-LoS) setting with a TX-RX separation of 15 m. The results we report are for 100 channel realizations obtained from the channel simulator. The channel matrix for each realization is scaled so that the expected Frobenius norm of the channel, i.e., $\mathbb{E}[\|\mathbf{H}\|_F^2]$, is N^2 . The SNR in the channel measurements in (1) is defined as SNR = $10 \log_{10}(1/\sigma^2)$. In this paper, we set $\sigma = 1$ so that the SNR during channel acquisition is 0 dB, and acquire M=126 channel measurements. The number of channel measurements chosen corresponds to a subsampling ratio of about 3% when compared to exhaustive scan.

The resolution of the oscillators at the TX and the RX is assumed to be within 20 ppm of the carrier frequency [3]. As a result, the maximum analog domain CFO in the system is 40 ppm of 38 GHz, i.e., $\Delta f=1.52\,\mathrm{MHz}$. In the digital domain, this translates to a maximum limit of $\Delta=0.096\,\mathrm{rad}$. As Δ is not exactly an integer multiple of $2\pi/N$, we define $u=\mathrm{ceil}(N\Delta/(2\pi))$. For the settings in our simulations, it can be observed that u=1. The channel measurements in our framework are acquired by applying different circulant shifts of a ZC sequence z to the phased arrays at the TX and the RX. The amount of circulant shifts to be used in the transceiver are determined by Algorithm 1. The root of the ZC sequence z is chosen as 11 so that its 3-bit phase quantized version preserves the unimodular DFT property [12].

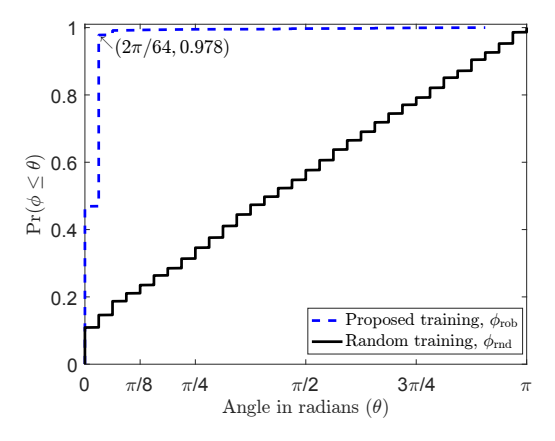


Fig. 2. Standard CS with the proposed training results in smaller beam misalignments when compared to IID random phase shift-based CS. Here, $\Delta f = 0.7812\,\mathrm{MHz}$ and $\mathrm{SNR} = 0\,\mathrm{dB}$.

To study the robustness of the proposed CS technique to CFO, we use OMP algorithm [17] to obtain the sparse channel estimate. Here, we choose a maximally off-grid CFO corresponding to a grid resolution of $2\pi/N$. Specifically, a CFO of 20.5579 ppm of the carrier frequency is considered so that $\epsilon=\pi/N$ and $n_\epsilon=0.5$. Under a CFO error, let $\hat{\mathbf{S}}_{\mathrm{rob}}$ and $\hat{\mathbf{X}}_{\mathrm{rnd}}$ denote the channel estimates obtained using OMP with the proposed training in Algorithm 1 and the IID random phase shift-based training in [7]. In both cases, the 2D-DFT basis was used for a sparse channel representation, and M=126 channel measurements were acquired at an SNR of $0\,\mathrm{dB}$. Then, the

coordinates where \mathbf{S} , $\hat{\mathbf{S}}_{\mathrm{rob}}$, and $\hat{\mathbf{X}}_{\mathrm{rnd}}$ achieve their maximum are determined. These coordinates are denoted by $(r_{\mathrm{opt}}, c_{\mathrm{opt}}), (r_{\mathrm{est}}, c_{\mathrm{est}})$, and $(r_{\mathrm{rnd}}, c_{\mathrm{rnd}})$. The deviations in the directional beams at the RX with the proposed training and the random training are computed as $\phi_{\mathrm{rob}} = 2\pi |r_{\mathrm{est}} - r_{\mathrm{opt}}|/N$ and $\phi_{\mathrm{rnd}} = 2\pi |r_{\mathrm{rnd}} - r_{\mathrm{opt}}|/N$. From the empirical cumulative distribution function of ϕ_{rob} and ϕ_{rnd} in Fig. 2, it can be observed that CS with IID phase shift based-training results in arbitrary beam misalignments under a CFO error. In contrast, CS using the proposed acquisition technique, i.e., Algorithm 1, results in beam misalignments within $2\pi/N$ of the best direction, highlighting the robustness achieved by our design.

Now, we evaluate the proposed technique with the beam broadening strategy in Sec. 3.3 using u=1 and $(r_{\rm est},c_{\rm est})$. The SNR with the broadened beams is shown as a function of CFO in Fig. 3. For the random phase shift-based training, the SNR is determined using directional beams corresponding to $(r_{\rm rnd}, c_{\rm rnd})$, i.e., $SNR_{rnd} = |\mathbf{X}(r_{rnd}, c_{rnd})|^2/\sigma^2$. For a benchmark, we evaluate Agile-Link [4], a non-coherent algorithm, under the same settings. As Agile-Link ignores the phase of the channel measurements, its performance is invariant to CFO. We set the TX and RX bin parameters in Agile-Link to 4, and use 8 hashes to obtain 128 channel measurements. From Fig. 3, it can be observed that standard CS with random phase shift-based training fails beyond a CFO of 12.5 ppm. The proposed beam alignment technique that performs CCS using localized random subsampling followed by beam broadening achieves a reasonable SNR over a wider range of CFO, i.e., from $-40 \,\mathrm{ppm}$ to $40 \,\mathrm{ppm}$. It can be noticed from Fig. 3 that our approach does not perform as good as IID phase shift-based CS for $\epsilon = 0$. This reduction in SNR is due to the beam broadening strategy that ensures robustness to any unknown CFO within 40 ppm.

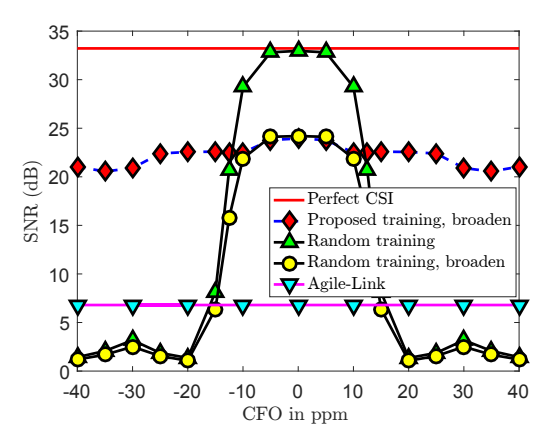


Fig. 3. The proposed beam broadening strategy corrects small beam misalignments after CS using our new training, and achieves a reasonable SNR over a wide range of CFO. It can be observed that IID random phase shift-based CS results in large beam misalignments that cannot be corrected using the same beam broadening strategy.

5. CONCLUSIONS AND FUTURE WORK

We have proposed a new sampling technique for CS-based beam alignment that achieves robustness to unknown phase errors due to CFO. The directional beams obtained using our method differ from the best ones only by a small amount when compared to standard random designs. Using a beam broadening strategy, we showed that a reasonably high SNR can be achieved with our approach even when standard techniques fail. Extending our idea to generic robust CS problems is an interesting direction for future work.

6. REFERENCES

- [1] S. Rangan, T. S. Rappaport, and E. Erkip, "Millimeter-wave cellular wireless networks: Potentials and challenges," *in Proc. of the IEEE*, vol. 102, no. 3, pp. 366–385, 2014.
- [2] R. W. Heath, N. Gonzalez-Prelcic, S. Rangan, W. Roh, and A. M. Sayeed, "An overview of signal processing techniques for millimeter wave MIMO systems," *IEEE J. Sel. Topics Signal Process.*, vol. 10, no. 3, pp. 436–453, 2016.
- [3] T. Nitsche, C. Cordeiro, A. B. Flores, E. W. Knightly, E. Perahia, and J. C. Widmer, "IEEE 802.11 ad: directional 60 GHz communication for multi-gigabit-per-second wi-fi," *IEEE Commun. Mag.*, vol. 52, no. 12, pp. 132–141, 2014.
- [4] O. Abari, H. Hassanieh, M. Rodreguez, and D. Katabi, "Millimeter wave communications: From point-to-point links to agile network connections," in *Proc. of the ACM Workshop on Hot Topics in Networks*, 2016, pp. 169–175.
- [5] E. J. Candès and M. B. Wakin, "An introduction to compressive sampling," *IEEE Signal Process. Mag.*, vol. 25, no. 2, pp. 21– 30, 2008.
- [6] Z. Marzi, D. Ramasamy, and U. Madhow, "Compressive channel estimation and tracking for large arrays in mm-wave picocells," *IEEE J. Sel. Topics Signal Process.*, vol. 10, no. 3, pp. 514–527, 2016.
- [7] J. Rodríguez-Fernández, N. González-Prelcic, K. Venugopal, and R. W. Heath Jr, "Frequency-domain compressive channel estimation for frequency-selective hybrid mmWave MIMO systems," *IEEE Trans. Wireless Commun.*, vol. 17, no. 5, pp. 2946–2960, 2018.
- [8] N. J. Myers and R. W. Heath Jr, "A compressive channel estimation technique robust to synchronization impairments," in Proc. of the IEEE Signal Process. Adv. Wireless Commun. (SPAWC), 2017.

- [9] J. Brady, N. Behdad, and A. M. Sayeed, "Beamspace MIMO for millimeter-wave communications: System architecture, modeling, analysis, and measurements," *IEEE Trans. Anten*nas and Propagation, vol. 61, no. 7, pp. 3814–3827, 2013.
- [10] K. Li, L. Gan, and C. Ling, "Convolutional compressed sensing using deterministic sequences," *IEEE Trans. Signal Process.*, vol. 61, no. 3, pp. 740–752, 2013.
- [11] N. J. Myers, A. Mezghani, and R. W. Heath Jr, "Spatial Zadoff-Chu modulation for rapid beam alignment in mmwave phased arrays," in *Proc. of the IEEE Global Telecommun. Conf.* (GLOBECOM), 2018.
- [12] —, "Swift-Link: A compressive beam alignment algorithm for practical mmwave radios," *arXiv preprint arXiv:1806.2005v2*, 2018.
- [13] E. J. Candès, J. Romberg, and T. Tao, "Robust uncertainty principles: Exact signal reconstruction from highly incomplete frequency information," *IEEE Trans. Inform. Theory*, vol. 52, no. 2, pp. 489–509, 2006.
- [14] A. C. Kak and M. Slaney, Principles of computerized tomographic imaging. IEEE press, 1998.
- [15] P. Stoica, H. He, and J. Li, "New algorithms for designing unimodular sequences with good correlation properties," *IEEE Trans. on Signal Process.*, vol. 57, no. 4, pp. 1415–1425, 2009.
- [16] S. Sun, G. R. MacCartney Jr, and T. S. Rappaport, "A novel millimeter-wave channel simulator and applications for 5G wireless communications," arXiv preprint arXiv:1703.08232, 2017.
- [17] J. Wang, S. Kwon, and B. Shim, "Generalized orthogonal matching pursuit," *IEEE Trans. Signal Process.*, vol. 60, no. 12, pp. 6202–6216, 2012.